Universiteit Utrecht

Comparing hydrodynamics to electrodynamics to find the translational friction tensor

Author:
Gijs BOOSTEN

Supervisor:
Prof. Dr. Marjolein DIJKSTRA

June 15, 2013

2

Abstract

Experimentalist are getting better control over the shape of nanoparticles and, as a result, particles of various shapes have become available. These particles are becoming more anisotropic. Where we used coefficients for years we now have to turn to tensors to describe the properties of the particles. One of the interesting propertierties is the diffusion coefficient, which now becomes the diffusion tensor. The diffusion tensor is inversely proportional to the friction tensor. In recent papers the analogy between hydrodynamics and electrodynamic has been described and in this research we try to find the analogy of the coupled dipole method in electrodynamics to calculate the translational friction tensor in hydrodynamics. In hydrodynamics we call this the bead model theory, with which we can successfully describe the translational friction tensor. The bead model theory is almost identical to the coupled dipole method, only the interaction tensors differ. We make a model for the coupled dipole method and the bead model system where we only interchange the interaction tensors. We have shown that the models work correctly by comparing them to recent papers and finally we compared the results for differently shaped particles. Unfortunately we cannot use the results of the coupled dipole method to calculate the friction tensor. However in this research we have shown that both methods are similar except for the interaction tensor. In the future we can adjust the coupled dipole method models to hydrodynamic models, just by changing the interaction tensor.

Contents

Chapter 1

Introduction

Nanoparticles are a hot topic in modern-day physics. While it was not possible to grow spherically shaped nanoparticles a few years ago, we now can tune the size within a few nanometer. The field of colloid science is evolving rapidly, which has resulted in an enormous variety of particle shapes that are available now experimentally [1]. In order to keep up with experimental physics, computer simulation groups have to use anisotropic particles as well, which come with new difficulties. We can for instance not apply rotational symmetry any more, and we have to use tensors to model many of the properties of our colloid particles. One of the properties of a colloid is the diffusion coefficient, which turns into a diffusion tensor for an anisotropic particle. It turns out to be very hard to determine the diffusion tensor from theory or experiments, so we have to turn to approximations and simulations in order to determine these tensors.

In this thesis I try to determine the diffusion coefficient for an arbitrary shaped particle using the bead model theory. An analogous model is widely used in electrodynamics and known as the Coupled Dipole Method (CDM). In this thesis, I will try to find a relationship between the CDM in electrodynamics and the bead model theory in hydrodynamics. If there is a relationship we can use the results from the CDM simulations to determine the diffusion tensors in hydrodynamics.

In the first chapter I will describe the theory of hydrodynamics and electrodynamics. I start off with the simplest case of a spherical particle in an ideal fluid or in a static electric field. We describe the solutions and find a relationship between electrodynamics and hydrodynamics. Next I turn to a non ideal fluid and derive the Stokes coefficient, which I then use to describe the bead model system. After describing the CDM, I can compare the two models with each other. In the second chapter I will describe the model used to study the CDM and bead model system in more detail. I will show how to make the particles out of beads and then show how to build up the matrix. In the third chapter the results from the model for cuboids and cylinders are described for both the CDM and the bead model system. Furthermore we compare two methods of building up particles out of beads and determine which method works better. In the last chapter we summarize the results and try to answer the main question of this bachelor project. In the end we propose some future research projects on this subject.

Chapter 2

Theory

In this chapter the theory of both electrodynamics and hydrodynamics will be described. I will first describe both cases separately in different sections and then I compare them to each other to see if it is possible to link them together.

2.1 Ideal flow field versus static electric field around a sphere

Before we turn our attention to the theory of the bead model system or the CDM we start off by comparing simple hydrodynamics with electrodynamics. This way we can see if there is a relationship between hydrodynamics and electrodynamics.

An object in a flow field appears to be very similar to a dielectric in a continuum subjected to an electric field. To illustrate the mapping, we discuss in detail a dielectric sphere in an electric field and a sphere in a flow field. Subsequently, we want to extend the mappings to anisotropic particles. In both cases the problem reduces to solving the Laplace equations with specific boundary conditions.
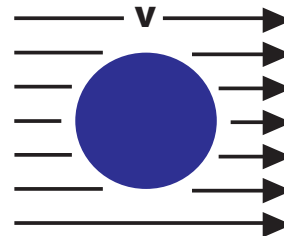

Figure 2.1: *Flow field past an object, with* **v** *the velocity of the flow.*

2.1.1 Fluid dynamics

If we want to describe the flow of an ideal fluid we have to derive the fundamental equation of fluid dynamics, the continuity equation. Let us begin by writing down the equation for the conservation of matter. $\int_{V_0} \rho dV$, where ρ is the fluid density and V_0 a volume element. Next, the flow through a volume element V_0 is given by $\rho \mathbf{v} \cdot d\mathbf{f}$, with df a surface element and v the velocity of the fluid. By convention we take $\rho \mathbf{v} \cdot d\mathbf{f}$ to be positive when the fluid flows out of our volume V_0 and negative if the fluid is flowing into the volume V_0. The total mass flowing out of the volume V_0 in unit time is given by

$$\oint_{\partial V_0} \rho \mathbf{v} \cdot d\mathbf{f} \tag{2.1}$$

where we integrate over the the closed surface ∂V_0 surrounding the volume V_0. The decrease per unit time in mass of fluid in the volume V_0 is given by $-\frac{\partial}{\partial t} \int \rho dV$. The two terms should be

equal to each other, $\oint \rho \mathbf{v} \cdot d\mathbf{f} = -\frac{\partial}{\partial t} \int \rho dV$. If we now transform the surface integral by Green's formula to a volume integral and see that it should hold for any volume V_0, we get the equation of continuity:

$$\frac{\partial \rho}{\partial t} + \nabla(\rho \mathbf{v}) = 0 \tag{2.2}$$

Figure 2.2: *Spherical coordinates, here ϕ is the angle between the x and y axis en θ is the angle between z and the vector $\mathbf{r}$.*

From the equation of continuity we cannot determine the velocity yet; we need to derive another set of equations, the Euler equations for an ideal fluid. Let us consider some volume in the fluid. The total force acting on this volume is equal to $-\oint pd\mathbf{f}$, the integral of the pressure over the boundary of the volume. Using Green's formula, we can transform this to a volume integral, $-\oint pd\mathbf{f} = -\int \nabla pdV$. We can then write the equation of motion of a volume element in the fluid by equating the force to the product of density times accaleration.
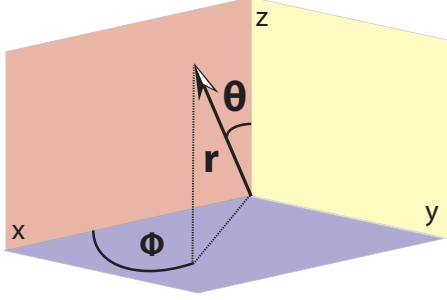
$$\rho \frac{d\mathbf{v}}{dt} = -\nabla p \tag{2.3}$$

We look at a particle in a fluid, so the accaleration consits of two components, namely te change in velocity at a point fixed in space, and the difference between the velocities at two points d$\mathbf{r}$ apart. So $\frac{d\mathbf{v}}{dt} = \frac{\partial \mathbf{v}}{\partial t} + (\mathbf{v} \cdot \nabla)\mathbf{v}$. If we substitute this back into Eq.2.3 we get Eulers equation.

$$\frac{\partial \mathbf{v}}{\partial t} + (\mathbf{v} \cdot \nabla)\mathbf{v} = -\frac{1}{\rho}\nabla p \tag{2.4}$$

We need one more equation to describe the flow correctly, and that is the adiabatic equation. Since there is no heat transfer between different parts of the fluid, we have indeed an adiabatic equation. In the case of an ideal fluid this means that the entropy is constant. From the first law of thermodynamics we then know $dw = Vdp$, where w is the heat function per unit mass, and $V = \frac{1}{\rho}$. Therefore $dw = \frac{dp}{\rho}$ and we can rewrite this a $\frac{\nabla p}{\rho} = \nabla w$ and put this back into 2.4.

$$\frac{\partial \mathbf{v}}{\partial t} + (\mathbf{v} \cdot \nabla)\mathbf{v} = -\nabla w \tag{2.5}$$

We can now use the well known relationship in vector analysis

$$\frac{1}{2}\nabla v^2 = \mathbf{v} \times (\nabla \times \mathbf{v}) + (\mathbf{v} \cdot \nabla)\mathbf{v}$$

We can use this formula to rewrite Eq.2.5 and take the curl on both sides to obtain an Euler equation which only involves the velocity,

$$\frac{\partial}{\partial t}\nabla \times \mathbf{v} = \nabla \times (\mathbf{v} \times (\nabla \times \mathbf{v})). \tag{2.6}$$

We can use the equation of continuity and Euler's equation to find a solution for the velocity for an incompressible ideal fluid, where ρ is constant. This means, the continuity equation reduces to $\nabla \mathbf{v} = 0$. A vectorfield with vanashing curl can be written as the gradient of a scalar field Φ, i.e. $\mathbf{v} = \nabla \Phi$. Therefore if we take $\mathbf{v} = \nabla \mathbf{\Phi}$, we get $\nabla \times \mathbf{v} = \nabla \times \nabla \Phi = 0$. We call Φ the potential flow, and if we put this back into the continuity equation equation we get the Laplace equation.

$$\nabla^2 \mathbf{\Phi} = 0 \tag{2.7}$$

With this equation we can describe an object in an ideal incompressible flow field. Suppose our fluid moves with constant velocity in the z direction $\mathbf{v_0} = v_0 \hat{z}$, then our potential flow field has to satisfy $\Phi \to \mathbf{v} r \cos(\theta)$ if $r \to \infty$, in spherical coordinates (see Fig: 2.2).

We know that solutions (in spherical coordinates) of the Laplace equation, that vanish at infinity equals

$$\Phi_0 = -\frac{a}{r} + \mathbf{A} \cdot \nabla \frac{1}{r} + \dots$$

Here the constant a and the tensor $\mathbf{A}$ are independent of the coordinates and depend on the shape of our particle, and we neglect higher order terms. Suppose we just use a firstorder approximation. Then the potential flow becomes $\mathbf{\Phi}_0 = -\frac{a}{r}$, such that we have for our velocity $\mathbf{v} = \nabla \mathbf{\Phi}_0 = a\frac{\mathbf{r}}{r^3}$. Now we calculate the flow around a closed surface, say a sphere with radius R. On the surface the velocity is constant and since we cannot have fluid flowing into the sphere this must be zero. The flow past a sphere is given by $\rho \mathbf{v}_R 4\pi R^2 = 4\pi \rho a$ and this can only be zero if $a = 0$. We now obtain for the potential flow the following equation

$$\Phi = \frac{\mathbf{A} \cdot \hat{r}}{r^2} + v_0 r \cos(\theta) \tag{2.8}$$

From the potential flow, we obtain the velocity of the fluid, in general this is given by

$$\mathbf{v} = \nabla \Phi = \nabla (\mathbf{A} \cdot \nabla \frac{1}{r} + v_0 r \cos(\theta)) = \frac{3(\mathbf{A} \cdot \hat{r})\hat{r} - \mathbf{A}}{r^3} + \mathbf{v_0}$$

We can calculate $\mathbf{A}$ for a sphere. We have an impenetrable object and therefore the fluid cannot go through the surface of our object and we use the kinematic boundary conditions. Kinematic boundary conditions state that the velocity of the fluid on the surface of the particle is zero. In our situation, where the particle has no velocity the fluid should come at rest at the surface of our object, so

$$\mathbf{v} \cdot \mathbf{n} = \nabla \Phi \cdot \hat{n} = \frac{\partial \Phi}{\partial \hat{n}} = 0.$$

Now we can compute the potential velocity for a sphere. We see that the normal vector $\hat{n}$ is just equal to $\hat{r}$. So we can take the derivative with respect to r. This gives us $\mathbf{A} = \frac{R^3}{2} v_0 \cos(\theta) \mathbb{I}$ and we can put this back into the equation just derrived for the potential flow and the velocity in spherical coordinates:

$$\Phi = v_0 \cos(\theta)(r + \frac{R^3}{2r^2}) \tag{2.9}$$

$$\left. \begin{array}{l} v_r = v_0 \cos(\theta)(1 - \frac{R^3}{r^3}) \\ v_\theta = -v_0 \sin(\theta)(1 + \frac{R^3}{2r^3}) \\ v_\phi = 0 \end{array} \right\}$$
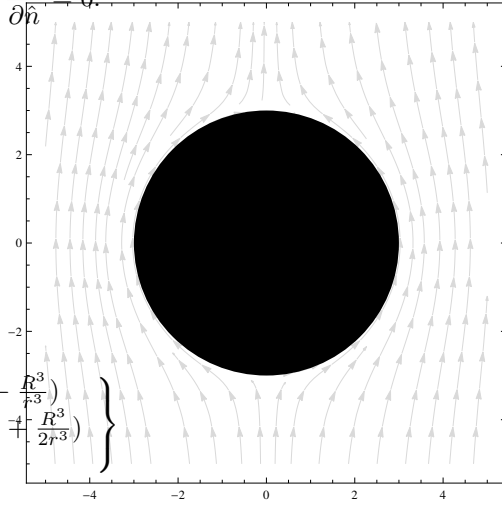

Figure 2.3: *Ideal fluid flow past a sphere in the $y = 0$ plane. We clearly see that the fluid goes around the sphere.*

2.1.2 Electrodynamics

Now we consider a similar problem in electrodynamics. We
have a linear dielectric sphere placed into a uniform electric field
($\mathbf{E} = E_0\hat{z}$), we know that any net charge must reside at the sur-
face [4]. Within such a dielectric, the potential obeys the Poisson
equation ($\nabla^2 V = -4\pi\rho$), with certain boundary conditions. We
have a dielectric without any charge, both inside and outside the
particle, so the Poisson equation reduces to the Laplace equa-
tion. Therefore we can solve the Laplace equation in two parts;
$V_{in}(r,\theta)$, when $r \leq R$ and for $V_{out}(r,\theta)$, when $r > R$. We need
to solve it with these boundary conditions.

Figure 2.4: *We have an
electric field (*$\mathbf{E}$*) within a
medium with dielectric con-
stant* ϵ_1*, within this medium
there is an object with dielec-
tric constant* ϵ_2*.*

(i)
$$V_{in} = V_{out}, \qquad \text{at} \quad r = R \tag{2.10}$$

(ii)
$$\epsilon_2 \frac{\partial V_{in}}{\partial r} = \epsilon_1 \frac{\partial V_{out}}{\partial r} \qquad \text{at} \qquad r = R \tag{2.11}$$

(iii)
$$V_{out} \rightarrow -E_0 r \cos\theta \qquad \text{for} \qquad r \gg R \tag{2.12}$$

Sphere

Now we have these boundary conditions we can start solving the Laplace equation for a sphere. [4]
The general solution for the Laplace equation in spherical coordinates is, with P_l the Legendre
polynomials.

$$V(r,\theta) = \sum_{l=0}^{\infty} (A_l r^l + \frac{B_l}{r^{l+1}}) P_l(\cos(\theta)) \qquad P_l \quad \text{are the Legendre Polynomials} \tag{2.13}$$

We see that if B_l is not zero within the sphere this term will blow up, therefore we obtain the
general solution within the sphere as $V_{in}(r,\theta) = \sum_{l=0}^{\infty} (A_l r^l) P_l(\cos(\theta))$. According to Eq.2.12 we
find outside the sphere $V(r,\theta) = \sum_{l=0}^{\infty} (\frac{B_l}{r^{l+1}}) P_l(\cos(\theta)) - E_0 r \cos(\theta)$. Now we have the two general
solutions to our problem. We can use the other boundary conditions to find the exact solutions.
From Eq.2.11 we find that $\sum_{l=0}^{\infty} (A_l R^l) P_l(\cos(\theta)) = \sum_{l=0}^{\infty} (\frac{B_l}{R^{l+1}}) P_l(\cos(\theta)) - E_0 R \cos(\theta)$. so[1]

$$\left.\begin{array}{l} A_l R^l = \frac{B_l}{R^{l+1}}, \qquad \text{for} \qquad l \neq 1 \\[2mm] A_1 R = -E_0 R + \frac{B_1}{R^2} \end{array}\right\} \tag{2.14}$$

Meanwhile, condition 2.11 yields (with $\epsilon_r = \frac{\epsilon_1}{\epsilon_2}$):

$$\epsilon_r \sum_{l=0}^{\infty} (A_l l R^{l-1}) P_l(\cos(\theta)) = -E_0 \cos(\theta) + \sum_{l=0}^{\infty} (\frac{(l+1)B_l}{R^{l+2}}) P_l(\cos(\theta)) \tag{2.15}$$

---

[1]The coefficients must be equal for each l, as you could prove by multiplying by $P_{l'}(\cos(\theta))\sin(\theta)$ and integrating
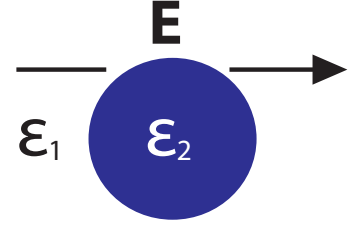from 0 to π, and using the orthogonality of the Legendre polynomials.

Then it follows that:

$$\left.\begin{array}{ll} A_l = B_l = 0, & \text{for} \quad l \neq 1 \\ A_1 = -\frac{3}{\epsilon_r+2}E_0 & B_1 = \frac{\epsilon_r-1}{\epsilon_r+2}R^3 E_0 \end{array}\right\} \tag{2.16}$$

Therefore we have the following solution to the potentials:

$$\left.\begin{array}{l} V_{in}(r,\theta) = -\frac{3}{\epsilon_r+2}E_0 r\cos(\theta) = -\frac{3}{\epsilon_r+2}E_0 z \\ V_{out}(r,\theta) = \frac{\epsilon_r-1}{\epsilon_r+2}\frac{R^3}{r^2}\cos(\theta)E_0 - E_0 r\cos(\theta) \end{array}\right\} \tag{2.17}$$

We can generalize these equations for any direction of the electric field, the third boundary condition 2.12 changes to $V = -\int \mathbf{E}dr$ if $r \gg R$, and we obtain the following solution:

$$V_{out}(r,\theta) = \frac{\epsilon_r-1}{\epsilon_r+2}\frac{R^3}{r^2}\mathbf{E}\cdot\hat{r} - \mathbf{E}\cdot\hat{r} \tag{2.18}$$

Next we have two cases we can determine, first we compute the electric field inside the sphere. We know that $\mathbf{E} = -\nabla V$, so here we have the electric field inside the sphere:

$$\mathbf{E} = \frac{3}{\epsilon_r+2}\mathbf{E}_0 \tag{2.19}$$

We can also determine the electric field outside the sphere, which gives:

$$\left.\begin{array}{l} E_r = E_0\cos(\theta)(-1 + \frac{\epsilon_r-1}{\epsilon_r+2}\frac{2R^3}{r^3}) \\ E_\theta = -E_0\sin(\theta)(1 - \frac{\epsilon_r-1}{\epsilon_r+2}\frac{R^3}{2r^3}) \\ E_\phi = 0 \end{array}\right\}$$

For the potential outside the sphere we see that the $E_0 r\cos(\theta)$ term is precisely the term which comes from the original electric field, therefore we have the correction term $\frac{\epsilon_r-1}{\epsilon_r+2}\frac{R^3}{r^2}\cos(\theta)E_0$ which is attributable to the dielectric, because we have a $\frac{1}{r^2}$ term the dielectric causes a dipole contribution to the electric field.

Figure 2.5: *Electric field past a sphere in the plane y=0. Because of the boundary conditions we have the flow going into the sphere, where there is a constant electric field.*

Dipole

If we look into the theory of dipoles, we find the following general term for the potential.

$$V_{dip} = \frac{1}{4\pi\epsilon_0}\frac{\mathbf{p}\cdot\hat{r}}{r^2} \qquad \mathbf{p} \equiv \int \mathbf{r}'\rho(\mathbf{r}')dr' \tag{2.20}$$

In our previous example we see that we have a dipole moment given by [8]:

$$\mathbf{p} = 4\pi R^3\frac{\epsilon_r-1}{\epsilon_r+2}\mathbf{E}_0 \tag{2.21}$$

Since the difinition of the electric polarizabillity (α) is given by: $\mathbf{p} \equiv \alpha\mathbf{E}$, we have

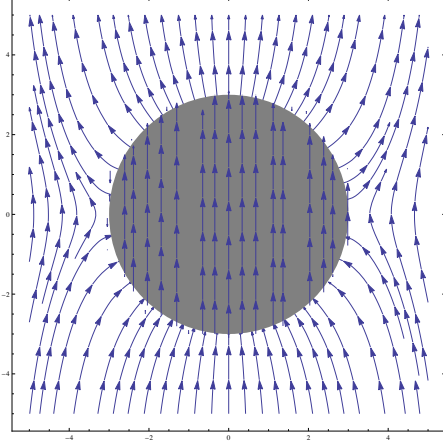$$\alpha = 4\pi\epsilon_0 R^3\frac{\epsilon_r-1}{\epsilon_r+2} \tag{2.22}$$

2.1.3   Mapping

Now we can make the comparison between the theory of hydrodynamics and electrodynamics. In both the cases we have to solve the Laplace equations, with certain boundary conditions:

Hydrodynamics	Electrodynamics
Laplace equations $\nabla^2 \Phi = 0$	*Laplace equations* $\nabla^2 V = 0$
Boundary conditions $\nabla \Phi = \mathbf{v}$ $\mathbf{v} \to \mathbf{v_0} \quad$ if $\quad r \gg R$ $\mathbf{v} \cdot \hat{n} = 0$ at boundary	*Boundary conditions* $\nabla V = -\mathbf{E}$ $\mathbf{E} \to \mathbf{E_0} \quad$ if $\quad r \gg R$ $\epsilon_1 \frac{\partial V_{in}}{\partial r} = \epsilon_2 \frac{\partial V_{out}}{\partial r} \quad$ at boundary $V_{in} = V_{out}, \quad$ at boundary
Solutions for a sphere $\Phi = v_0 \cos(\theta)(r + \frac{R^3}{2r^2})$	*Solutions for a sphere* $V_{out}(r,\theta) = E_0 \cos(\theta)(\frac{\epsilon_r - 1}{\epsilon_r + 2}\frac{R^3}{r^2} - r)$

We see that both solutions look quite similar. There is both an r and a $\frac{1}{r^2}$ term involved. But for the hydrodynamic solution both terms are positive, while for the electrodynamic solution we have oposite signs. Therefore as we saw in earlier sections the flow goes around the sphere (same signs), while the electric field goes into the sphere (differents signs).

Nevertheless if we take $\mathbf{E}$ as an analogy of $\mathbf{v}$, we get $\nabla \phi = \mathbf{v} <=> \mathbf{E} = -\nabla V$. Therefore the best thing to do is take $\mathbf{v} <=> -\mathbf{E}$. Then we can also find an analogy between $\mathbf{A}$ and $\frac{\epsilon_r - 1}{\epsilon_r + 2} R^3 \mathbf{E}_0$. If we leave the original potential term aside (as we can do in both cases) we can write;

$$\mathbf{A} = -R^3 \frac{\epsilon_r - 1}{\epsilon_r + 2} \mathbf{E}_0 \tag{2.23}$$

If we now see $\mathbf{E}_0$ as the direction of the flow of the sphere we can treat it as $-\mathbf{v}$. We have found $\mathbf{A} = -\frac{R^3}{2}\mathbf{v_0}$, so if $\frac{\epsilon_r - 1}{\epsilon_r + 2} <=> \frac{1}{2}$ we have an exact mapping.

We also recognize a r^{-3} in the velocity, which we know from the theory of dipoles. It would be a good idea to look into the theory of dipoles. For a dipole we have an electric field given by [4];

$$\mathbf{E} = \frac{1}{4\pi\epsilon_0} \frac{1}{r^3}[3(\mathbf{p} \cdot \hat{r})\hat{r} - \mathbf{p}] \tag{2.24}$$

Which looks similar to the change in velocity described in the first section of the theory. We can make one final analogy between the dipole moment and $\mathbf{A}$.

$$\mathbf{A} <=> \frac{1}{4\pi\epsilon_0}\mathbf{p} = \alpha\mathbf{E}_0 \tag{2.25}$$

Therefore if we look at the polarizabillity factor we have $\alpha \equiv 4\pi\epsilon_0$ in this case.

2.2   Diffussion Tensor

In this section we will derive an expression for the diffusion tensor in terms of the velocity and drag force of a particle. We start off with the Einstein equation, which is given by

$$\mathbf{D} = k_B T \mu. \tag{2.26}$$

Here, k_B is the Boltzmann constant, T the temperature and μ is the mobility, defined by the ratio between the drag velocity and the drag force. So we see that we have a relationship between the velocity of the flow around the particle and the force exerted on the particle, this is called the friction coefficient, which is in general given by

$$\mathbf{F} = \zeta \mathbf{v} \tag{2.27}$$

Here we see that ζ is a tensor and that ζ^{-1} is equivalent to μ. Therefore, calculating the diffusion tensor is essentially the same as calculating the friction tensor, which is in essence solving the Navier-Stokes equation for the velocity and for the force.

In many experiments the diffusion constant is used instead of the diffusion tensor. We can calculate this constant by taking $D = \frac{3k_B T}{\text{Tr}(\zeta)}$.

2.2.1 Friction coefficient of a sphere

In this section we will calculate the diffusion tensor for a sphere (which, in the case of a sphere, is a constant times the identity matrix). [7] We will start with solving the Navier-Stokes equation for a sphere. In the first section we already described the motion of a sphere in an ideal incompressible fluid. In this section we will generalize the above to a viscous fluid and derive the expression for the velocity and the expression for the force.

For an ideal fluid we have seen that the velocity of the fluid is described by three equations, the adiabatic equation, the Euler's equation and the the equation of continuity, the last is valid for all fluids. The adiabatic equation is not valid any more, since there can be momentum transfer between different parts in the fluid. We thus need to modify Euler's equation for a viscous fluid. We need to add terms to Eulers equations which describe the irreversible "viscous" transfer of momentum in the fluid. If we add those terms and assume that the viscosity is constant throughout the fluid we get the Navier-Stokes equation,

$$\rho[\frac{\partial \mathbf{v}}{\partial t} + (\mathbf{v} \cdot \nabla)\mathbf{v}] = -\nabla p + \eta \nabla^2 \mathbf{v} + (\zeta + \frac{1}{3}\eta)\nabla(\nabla \cdot \mathbf{v}). \tag{2.28}$$

Here ρ is the density of the fluid, the pressure p, the viscosity of the fluid η, and the second viscosity ζ. We now consider an incompressible fluid, therefore $\nabla \mathbf{v}$ is zero and the final term will vanish. With this in mind we can proceed to describe the flow around a sphere. To solve the Navier-Stokes equation exactly we consider here the flow with small Reynolds numbers. The Navier-Stokes equation for steady flow of an incompressible fluid is given by

$$(\mathbf{v} \cdot \nabla)\mathbf{v} = -\frac{1}{\rho}\nabla p + \frac{\eta}{\rho}\nabla^2 \mathbf{v} \tag{2.29}$$

We now know that the term $(\mathbf{v} \cdot \nabla)\mathbf{v}$ is in the order of magnitude $\frac{u^2}{l}$, where u is the velocity of the main stream and l the geometrical properties of the particle. Then the term on the right $\frac{\eta}{\rho}\nabla^2 \mathbf{v}$, is of the order of magnitude $\frac{\eta u}{\rho l^2}$. The Reynolds number is the ratio between the two, therefore given by

$$\frac{u\rho l}{\eta}. \tag{2.30}$$

If we have a flow with low Reynolds numbers, the inertia term is much smaller than the viscous term, and can therefore be neglected. The Navier-Stokes equation becomes linear and we find the following equation.

$$\eta \nabla^2 \mathbf{v} - \nabla p = 0 \tag{2.31}$$

Of course the continuity equation holds, therefore the divergence of the velocity of the fluid is zero. One more remark is that if we take the curl of Eq.2.31 we get $\nabla^2(\nabla \times \mathbf{v}) = 0$.

With these assumptions we can now look at a sphere in a moving viscous fluid. We consider that the fluid is moving with velocity $\mathbf{v}$ and the sphere is at rest. Now we use the coordinate system in which the sphere is fixed. From the continuity equation we know that $\nabla(\mathbf{v}) = 0$, so $\mathbf{v}$ can be expressed as the curl of some vector $\mathbf{A}$

$$\nabla \times \mathbf{A} = \mathbf{v} \tag{2.32}$$

with the curl of $\mathbf{A}$ to be $\mathbf{v}_0$. Since we are considering a sphere we have no other preferred direction then $\mathbf{v}_0$, therefore $\mathbf{v}_0$ must appear linearly in $\mathbf{A}$. This gives us $\mathbf{A} = f'(r)\mathbf{n} \times \mathbf{v}_0$. Here $\mathbf{n}$ is a unit vector parallel to the position vector $\mathbf{r}$. The origin is the center of our sphere. We take $f'(r)$ as a gradient of another function $f(r)$. we thus see using the fact that the sphere is fixed and $\mathbf{v}_0$ is constant

$$\mathbf{v} = \mathbf{v}_0 + \nabla \times \nabla \times (f\mathbf{v}_0) \tag{2.33}$$

Now we take once more the curl of the above equation and use the fact that $\nabla \times \mathbf{v} = -\nabla^2(f\mathbf{v}_0)$. Using the continuity equation we see that $\nabla^2(\nabla \times \mathbf{v}) = -\Delta^2(f\mathbf{v}_0) = (\Delta^2\nabla f) \times \mathbf{v}_0 = 0$. Since $\mathbf{v}_0$ is constant we must have

$$\Delta^2\nabla f = 0 \tag{2.34}$$

If we integrate this we get $\Delta^2 f = \text{constant} = 0$ This is zero, because the velocity difference between the fluid and the particle must vanish at infinity and also their derivatives.

We now have the fourth derivative of f, whilst the velocity is given in terms of the second derivative of f. We have then

$$\Delta^2 f \equiv \frac{1}{r^2}\frac{d}{dr}(r^2\frac{d}{dr})\Delta f = 0 \tag{2.35}$$

If we solve this we get $\Delta f = 2\frac{a}{r} + c$ where c must $\mathbf{v}_0$, since . We now are left with $\Delta f = 2\frac{a}{r} + \mathbf{v}_0$, which we can again solve and obtain

$$f = ar + \frac{b}{r} + \mathbf{v}_0 \tag{2.36}$$

Now we can substitute this back into equation (2.33) and we find for the velocity of the fluid:

$$\mathbf{v} = \mathbf{v}_0 - a\frac{\mathbf{v}_0 + \mathbf{n}(\mathbf{v}_0 \cdot \mathbf{n})}{r} + b\frac{3\mathbf{n}(\mathbf{v}_0 \cdot \mathbf{n}) - \mathbf{v}_0}{r^3} \tag{2.37}$$

From the boundary conditions we need to determine the constants a and b. The nonslip requirement states that the relative motion between the particle and the fluid should disappear at the surface of a rigid rigid particle, so at $(r = R)$ we have $\mathbf{v} = 0$

$$0 = \mathbf{v}_0(\frac{a}{R} + \frac{b}{R^3} - 1) + \mathbf{n}(\mathbf{v}_0 \cdot \mathbf{n})(-\frac{a}{R} + \frac{3b}{R^3}) \tag{2.38}$$

In order for this equation to hold for all $\mathbf{n}$, the terms proportional to $\mathbf{v}_0$ and $\mathbf{n}(\mathbf{v}_0 \cdot \mathbf{n})$ both need to vanish, so we now finally have $a = \frac{3}{4}R$ and $b = \frac{1}{4}R^3$:

$$f = \frac{3}{4}Rr + \frac{1}{4r}R^3 \tag{2.39}$$

$$\mathbf{v} = \mathbf{v}_0 - \frac{3}{4}R\frac{\mathbf{v}_0 + \mathbf{n}(\mathbf{v}_0 \cdot \mathbf{n})}{r} + \frac{1}{4}R^3\frac{3\mathbf{n}(\mathbf{v}_0 \cdot \mathbf{n}) - \mathbf{v}_0}{r^3} \tag{2.40}$$

We can now write this equation in spherical coordinates along the $\mathbf{v}_0$ direction:

$$v_r = v_0 \cos(\theta)[1 - \frac{3R}{2r} + \frac{R^3}{2r^3}]$$

$$v_\theta = -v_0 \sin(\theta)[1 - \frac{3R}{4r} - \frac{R^3}{4r^3}]$$

We see that if we let $r \to \infty$ we get the fluid to move with speed v_0 If we compare this to the ideal fluid we see that we get an additional term which goes as $\frac{1}{r}$.

We have that the velocity of our fluid, we can also calculate the pressure and then the force exerted on the sphere. We started the above calculation with the Navier-Stokes equation for low Reynolds numbers $\eta\nabla^2 v = \nabla p$. If we now replace Eq.2.33 into this equation we get $\nabla p = \eta\nabla^2(\mathbf{v}_0 + \nabla \times \nabla \times (f\mathbf{v}_0))$ This then becomes $\nabla p = \eta\mathbf{v}_0 \cdot \nabla^2 f + p_0$ Here p_0 is the pressure at infinity and we can replace f by Eq.2.39 and substitute to spherical coordinates, such that we get our final expression

$$p = \eta v_0 \cos(\theta)(\frac{-3R}{2r^2}) + p_0 \tag{2.41}$$

With the pressure and the velocity we can determine the drag force and then the derive Stoke's law. We start off by determining the force per unit area (σ) in the flow direction at position (r,θ) for all ϕ. We have a viscous stress part which is given by $-\eta(\frac{\partial v_\theta}{\partial r}|_{r=R} \sin(\theta))$, and a pressure stress term given by $-(p - p_0)_{r=R} \cos(\theta)$. If we fill in the pressure (Eq.2.41) and $(\frac{\partial v_\theta}{\partial r}|_{r=R})$ the we get

$$\sigma = \frac{3}{2}\frac{\eta v_0}{R} \tag{2.42}$$

Now we can calculate the force exerted by the flow on the sphere by $F = \int_S \sigma ds$, where we integrate over the surface of the sphere. Since σ is constant we just take it out of our integral which results in the following expression

$$F = \int_S \sigma ds = \sigma \int_S ds = 4\pi R^2 \times \frac{3}{2}\frac{\eta v_0}{R} = 6\pi\eta R v_0 \tag{2.43}$$

Now we have derived the Stokes relation or the friction coefficient of a sphere

$$\zeta = \frac{F}{v_0} = 6\pi\eta R \tag{2.44}$$

2.3   Bead Model

For other objects than a sphere, there are almost no analytical results for the friction or diffusion tensor available. There are however many ways to calculate numerically the components of the friction tensor. Most of these consist of building up the particle out of small spherical particles (beads) and since we know the friction tensor (or coefficient) of a sphere and the interaction of two beads in a fluid, we can relatively easily calculate the interaction between these beads. From the interactions between these beads we can derive the friction and diffusion tensor.

2.3.1   Computational calculation of the friction tensor

We can make a set of equations which describes the motion of each bead, and with all these equations, we can model our particle [9] [5]. We have already the relation between drag force and velocity $\mathbf{v} = \frac{1}{\zeta}\mathbf{F}$, and we can extend this relationship with the hydrodynamic interaction

tensor. Now let us assume we have N beads with radius R, we can describe the velocity of a bead in the following way, where $\mathbf{v}_i = (\mathbf{v}_{x_i}, \mathbf{v}_{y_i}, \mathbf{v}_{z_i})^t$.

$$\sum_{j=1}^{N} \mathbb{T}_{ij} \mathbf{F}_j = \mathbf{v}_i, i = 1, \ldots, N \tag{2.45}$$

In this equation the tensor $\mathbb{T}_{ij}$ is the hydrodynamic interaction tensor. This was first derived by Oseen in 1910 to describe incompressible viscous flow for low Reynolds numbers and is now used to approximate the interaction between the beads of a particle. [5]

$$\left.\begin{array}{l} \mathbb{T}_{ii} = \frac{1}{6\pi\eta R}\mathbb{1} \\[2mm] \mathbb{T}_{ij} = \frac{1}{8\pi\eta r_{i,j}}(\mathbb{1} + \frac{\mathbf{r}_{i,j}\mathbf{r}_{i,j}^t}{|r_{i,j}|^2}) \end{array}\right\}$$

Here $\mathbf{r}_{i.j} = \mathbf{r}_i - \mathbf{r}_j$ and $|\mathbf{r}_{i.j}|$ is the length of this vector. We are interested in the translational friction tensor, therefore all beads are moving with the same velocity in Cartesian coordinates, so $\mathbf{v}_i = \mathbf{v}$. The next step is to calculate the friction tensor with these equations

$$\sum_{j=1}^{N} \mathbb{T}_{ij} \mathbf{F}_j = \mathbf{v} \qquad \text{for} \qquad i = (1, 2, \ldots, N) \tag{2.46}$$

The only thing we have to do is to invert the $3N \times 3N$ matrix $\mathbb{T}$, which is build up from the 3×3 matrices $\mathbb{T}_{ij}$ to get our $3N$vector $\mathbf{F}$, which is built up out of the forces on the individual beads. Next we can use the simple relationship between force, velocity and friction coefficient (Eq.2.27). When we have the $3N$ vectors for the velocity and the force we can compute the friction tensor in the following way. We know, for the particle, that the sum on the forces on the individual beads equals the force on the particle.

$$\boldsymbol{\Xi} \equiv (\sum_{j=1}^{N} \mathbf{F}_j)\mathbf{v}^{-1} \tag{2.47}$$

2.3.2   Computational calculation of the polarization tensor

The polarization tensor of a particle can also be described by building a particle out of beads, in this case small dipoles and calculate the interaction between them. Here I will explain how this can be done. [3] If we have a cluster of beads and we place these beads in a static electric field, each bead develops an induced dipole moment that depends on both the applied field and the field caused by all the other beads. Therefore we cannot say the polarizabillity is just the sum of the polarizabillity of each bead. If we look at the local electric field ($\mathbf{E}_{loc}$), it is the sum of the static electric field and the effect caused by the beads, so it becomes

$$\mathbf{E}_{loc} = \mathbf{E}_0 + \mathbf{E}_{int,j} \tag{2.48}$$

$$\mathbf{E}_{int,j} = \mathbb{T}_{i,j} \cdot \mathbf{p}_j \tag{2.49}$$

$$\mathbb{T}_{i,j} = \sum_{\substack{j=1 \\ i \neq j}}^{N} \frac{1}{|r_{i,j}|^3}(3\frac{\mathbf{r}_{i,j}(\mathbf{r}_{i,j})^t}{|r_{i,j}|^2} - \mathbb{1}) \tag{2.50}$$

The $\mathbb{T}_{i,j}$ is called the dipole field tensor, and is known as the interaction tensor between two dipoles in electrodynamics. $\mathbf{p}_i$ is the induced dipole moment of bead i. The notation for $r_{i,j}$ is the same as in the hydrodynamic case. We want to know the total induced dipole moment of our cluster we can sum these dipole moments to get the total dipole moment. (p_t)

$$\mathbf{p}_t = \sum_{i=1}^{N} \mathbf{p}_i \tag{2.51}$$

We know that there is a relationship between the induced dipole moment and the electric field, namely the polarization, so for the particle we have, where α_t is the polarization tensor.

$$\mathbf{p}_t = \alpha_t \mathbf{E}_0 \tag{2.52}$$

We can also write this for each bead individually, where we have a constant polarization α_0

$$\mathbf{p}_j = \alpha_0 \mathbf{E}_j^{loc} \tag{2.53}$$

Now from equations 2.48, 2.49, 2.53 we get the following $3N$ linear equations, where $\mathbf{E}_0 = \mathbf{e}E_0$

$$\frac{\mathbf{p}_i}{\alpha_0 E_0} - \frac{1}{E_0}\mathbb{T}_{ij} \cdot \mathbf{p}_j = \mathbf{e}$$

If we define $T_{i,j}$ the same as in the hydrodynamic case and call it $T_{i,j}^*$

$$\left.\begin{array}{l} \mathbb{T}_{i,j}^* = \frac{1}{\alpha_0 E_0}\mathbb{1} \qquad \text{if} \quad i = j \\[2em] \mathbb{T}_{i,j}^* = \frac{1}{E_0|r_{i,j}|^3}\left(\mathbb{1} - \frac{3\mathbf{r}_{i,j}\mathbf{r}_{i,j}^t}{|r_{i,j}|^2}\right) \qquad \text{if} \quad i \neq j \end{array}\right\}$$

$$\sum_{j=1}^{N} \mathbb{T}_{ij}^* \cdot \mathbf{p}_j = \mathbf{e} \qquad \text{for} \qquad i = (1, 2, \ldots, N) \tag{2.54}$$

We can put these $3N$ linear equations into a matrix form and all we have to do is invert the $3N \times 3N$ $\mathbb{T}_{i,j}^*$ matrix to get the dipole moments $\mathbf{p}_j$ of our beads. If we have our $3N$ dipole vector $\mathbf{p}$, which consists out of the dipole moments from each bead, we can sum these individual dipole moments to get the polarizability.

$$\alpha_t \equiv \mathbf{p}_t \mathbf{E}_0^{-1} = \left(\sum_{j=1}^{N} \mathbf{p}_j\right)\mathbf{E}_0^{-1} \tag{2.55}$$

2.3.3 Similarities between polarization tensor and diffusion or friction tensor

In the previous sections we described the relation of both the hydrodynamic interaction tensor and the friction tensor and the electrodynamic interaction tensor and the polarizabitility. Both interaction tensors look quite similar.

Hydrodynamic

$$\mathbb{T}_{ii} = \frac{1}{6\pi\eta|r_i|}\mathbb{1}$$
$$\mathbb{T}_{ij} = \frac{1}{8\pi\eta|r_{i,j}|}\left(\mathbb{1} + \frac{\mathbf{r}_{i,j}\mathbf{r}_{i,j}^t}{|r_{i,j}|^2}\right)$$

Electrodynamic

$$\mathbb{T}_{ii}^* = \frac{1}{E_0\alpha_0}\mathbb{1}$$
$$\mathbb{T}_{i,j}^* = \frac{1}{E_0|r_{i,j}|^3}\left(\mathbb{1} - \frac{3\mathbf{r}_{i,j}\mathbf{r}_{i,j}^t}{|r_{i,j}|^2}\right)$$

There are two major differences between these tensors, namely the fact that the hydrodynamic tensor goes with the inverse of r and the electrodynamic interaction tensor with the inverse of r to the power three, furthermore we have a factor of three and a change of sign in the dipole interaction term. The change of signs is the same as we saw in the comparison between the ideal fluid flow and the electric field around a sphere.

Chapter 3

Model

The theory as explained in the previous section can be modeled by computer simulations. In this section I will explain the model step by step and also the additional theory needed to build this model.

3.1   Building up a particle out of beads

The first step is to build the particle out of small spherical beads, in order to apply the bead model theory. This can be done in various ways, but the easiest and most used way is to make a cubic lattice first and to cut out the shape of the desired particle. Of course the accuracy of our approximation depends heavily on the lattice size. We can however scale out the dimension of the lattice, then accuracy is then no longer dependent on the lattice size, but rather on the number of beads.

3.2   Cylinders

The first type of particles I use are cylinders, because these particles are relatively easy to model by beads. Here I describe how one can build up a cylinder in two different ways, the first is out of a square lattice as described above and the second theory is the Bresenham circle algorithm, which models the circles and therefore the cylinders better.

3.2.1   Square Lattice

The first type of particles we use are cylinders. The cylinders are built up in the following way: We start again with a square lattice with a lattice constant of 1, therefore the beads are non overlapping if the beads (spherically shaped) have a radius of 0.5. Next, we want to have a certain radius of our cylinder. This can be done by getting rid off the points, which are outside our desired radius. If we build up a lattice around the origin, this can be done by defining the points as $\{x, y, z\}$ and then $x^2 + y^2 \leq r^2$. We now have a disk in the xy plane, with radius r. The last step is to expand this radius to a cylinder by copying the x and y coordinates and let z coordinate run between 0 and $(L-1)$. The cylinder then has length L and diameter $2R$. In this
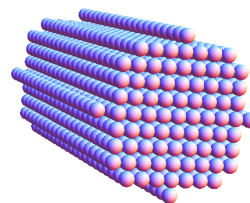

Figure 3.1: *Cylinder-shaped particle built up out of beads. Constructed from a square lattice, with lattice constant 1.*

19

way we can make any cylinder, with any length over diameter ratio, $\frac{L}{D}$.

3.2.2 Bresenham circles

Again our goal is to make a circle with radius r in the xy plane. We look at the first octant of a circle and apply the algorithm there. Then we copy, using the symmetry of the circle, the results to the other octants in order to complete the circle. We first draw a curve which starts at $(0, r)$ and makes the circle up to 45 deg . The coordinate of the first point $(n = 1)$ is $(0, r)$. Next we want to find the other points on this curve so we know the outer points of our circle. For each of these points (n) the circle

Figure 3.2: *On the left we see what happens if we just cut out a circle from a square lattice and right the bresenheim algorithm in action.*

equation holds $x_n^2 + y_n^2 = r^2$. This can be rearranged as $x_n^2 = r^2 - y_n^2$, and it holds for each n. We now proceed in finding the other points by moving up (positive direction) through y and occasionally move to the left in the x direction. With this in mind we can find the next coordinate by
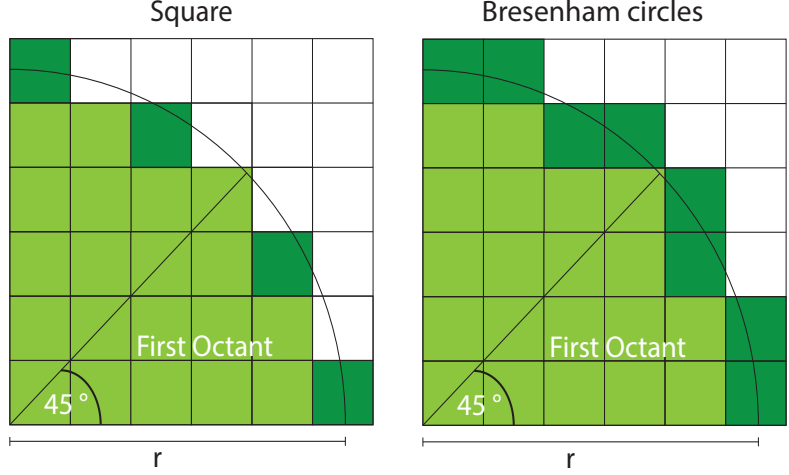
$$y_{n+1}^2 = (y_n + 1)^2 = y_n^2 + 2y_n + 1$$

$$x_{n+1}^2 = -y_{n+1}^2 + r^2 = -y_n^2 - 2y_n - 1 + r^2 = x_n^2 - 2y_n - 1$$

We have one problem left with this algorithm, which is that we have a lattice to work with. We therefore have to decide whether we accept the point or not. To do this we define an error parameter by;

$$ER(x_i, y_i) = |x_i^2 + y_i^2 - r^2|$$

Since we only compute the first octant we know that y always travels up and that x can only move one to the left in this move. Therefore we choose the least error as our best point, so if this expression is true we move x one to the left, and if it is false we leave x at the same place,

$$\text{ER}(x_i - 1, y_i + 1) < Er(x_i, y_i + 1) \tag{3.1}$$

Since a circle is symmetric we can copy the first octant to the other seven octants and find the outer part of our circle. When we have all the outer squares we only need to fill in the intermediate points. This can be done by starting from y_{-r} and move through all the x coordinates on that row and check whether $x^2 + y_{-r}^2 < x_{-r}^2 + y_{-r}^2$ is true and if this is true then fill in the square in this place. We then move up in the y direction and fill in all the squares and make a full circle. The procedure how to make a cylinder is the same as with the squares; we copy the x and y coordinates of the circle and change the z coordinate between 0 and $L - 1$. With this algorithm we can model the cylinder in a better way.

3.3 Model

Since we make our particle out of beads we have the coordinates of the center of each bead. The first step is to compute the interaction tensor ($\mathbb{T}$) between the beads, which give us a matrix of nine values. If we have a total number of n beads, we now have $9 * n^2$ values to keep, therefore if we increase our bead number by a factor of 2, we here have an increase of a factor 4 in data points. It is therefore important to model our particle with the least amount of beads, such that the calculation runs quickly. Next we have to put all these small interaction matrices $\mathbb{T}_{ij}$ into a matrix in the following way and we have our matrix equation for the hydrodynamic case ;

$$\begin{pmatrix} \mathbb{T}_{1,1} & \mathbb{T}_{1,2} & \cdots & \mathbb{T}_{1,n} \\ \mathbb{T}_{2,1} & \mathbb{T}_{2,2} & \cdots & \mathbb{T}_{2,n} \\ \vdots & \vdots & \ddots & \vdots \\ \mathbb{T}_{n,1} & \mathbb{T}_{n,2} & \cdots & \mathbb{T}_{n,n} \end{pmatrix} \begin{pmatrix} F_{1,x} \\ F_{1,y} \\ F_{1,z} \\ \vdots \\ F_{n,z} \end{pmatrix} = \begin{pmatrix} v_{1,x} \\ v_{1,y} \\ v_{1,z} \\ \vdots \\ v_{n,z} \end{pmatrix}$$

We now have a $3n \times 3n$ matrix times a $3n$ vector which is still unknown at this time. We can tune the velocity vector ourselves, and since we are looking for a translational friction tensor, the velocity is the same for each bead. The following, computationally heavy, step is to invert the huge $3n \times 3n$ matrix, where the fastest algorithm goes as $n^{2.3}$. Therefore the calculation of this model with more than 200 beads were not even computationally possible 1980 [2] and ten years ago simulations with more than 2000 beads were computationally hard [5]. With increasing computer power it is now possible to do simulations with $5.000 - 10.000$ beads. Nevertheless in this step it is also important to model the particle accurately, so we use the least amount of beads possible. When we compute the different components of the force (F_x, F_y, F_z) we can multiply it by $\{v_x, v_y, v_z\}^t$ to get our final translational friction tensor.

The difference between the hydrodynamic model and the electrodynamic model is the computations of the interaction tensors $\mathbb{T}_{i,j}$ as described in the theory. In the electrodynamic case the force becomes the dipole moment ($\mathbf{p}$) and the velocity is the static electric field $\mathbf{E}_0$. Besides those differences, the implemented models are identical.

Chapter 4

Results

In this chapter the numerical calculations of the computer simulations are presented. First I will ivestigate how accurate the CDM and bead model aproximations are with respect to the theory and then I check whether the Bresenham circle method indeed works better than the square method. Then the results of the the hydrodynamic model are shown for cuboids and cylindrically shaped particles. We continue with the electrodynamic model and see how the enhancement factor (polarizability divided by the sum of the individual polarizabilities of the beads) behaves for cuboids and for cylinder shaped particles. In the end we will compare the results for the electrodynamic and hydrodynamic theories.

4.1 Accuracy of the Model

I build both moddels as described in chapter 3 and we want to know how accurate the model is in comparison to the theory. For the hydrodynamic case we have derived the Stokes coefficient ($f = \frac{1}{6\eta\pi R}$) for a sphere. If we therefore model a sphere out of small beads and preform the bead model theory we expect to find the Stokes friction coefficient. So if we divide the numerically found data by the theoretical value we should get a dimensionless number of 1.

In electrodynamics we can do virually the same, but now for the polarizability. We first introduce the enhancement factor (f), which is the numerical value from the CDM (α) divided by the sum of the individual dipole moments ($n\alpha_0$), so ($f = \alpha/(\alpha_0 n)$). Here n is the number of beads. From theory we know that the polarizability of a sphere is the same as the sum of the individual dipole moments of the beads. Therefore we expect to find the dimensionless number 1 as well.

We can now preform the computations and check if the model represents the theory accurately.
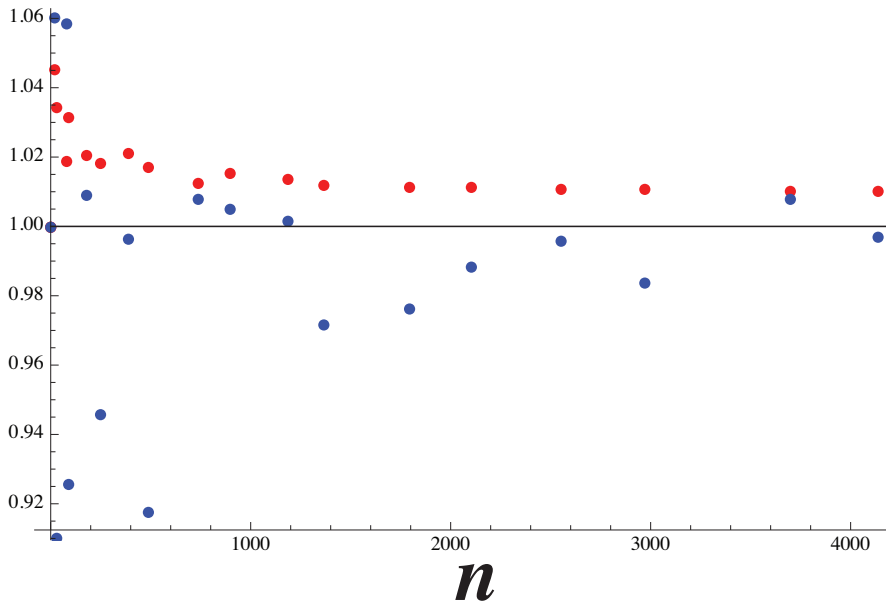
Figure 4.1: *In red we see the datapoints for the enhancement factor and in blue the datapoints for the friction coeffecient divided by the Stokes coefficient for different number of beads. We see that the datapoints for $n > 500$ are not really accurate, but if $n > 1000$ the values are in both cases accurate within 2% of the theoretical value and decreasing if n gets bigger. We see that the bead model is less accurate than the electrodynamic model, especially for a small radius (or less beads)*

4.2   Bresenham versus Square cylinders

In the model we have discussed two different ways to make a circle out of a square lattice. The first is to cut out a circle from a square lattice and take all the center of the beads which are inside the radius. The second way was to perform the Bresenham circle algorithm to find the outer beads and fill in the center part. We have computed different cylinders with the same $\frac{L}{D}$ ratio of 2. From these data we can see the Bresenham model is accurate for about 500 beads, so in our experiments with cylinders we should model them for at least 500 beads.

In Fig. 4.2, we plot the friction coefficient divided by the friction coefficient of a sphere with the same volume for cylinder shaped par-
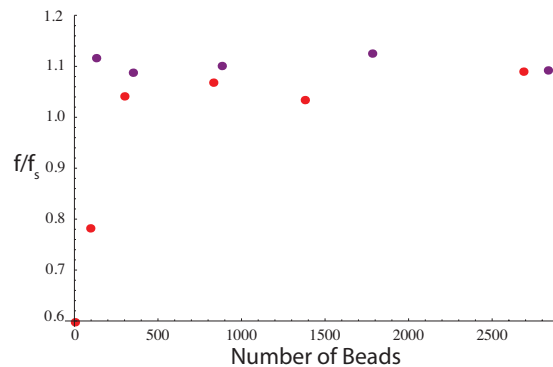

Figure 4.2: *The difference between the cylinders cut out of a square lattice (red) or the Bresenheim method purple). The calculated values are the mean friction coefficient (average of the ζ_i $i \in \{x, y, z\}$ of the friction tensor) divided by the stokes friction coefficient of a sphere with the same volume.*

ticles. The Bresenheim circles (in purple)
makes the modeled circles slightly bigger and therefore the mean translational component will
be slightly bigger than the true value. The square method models the cylinder smaller, therefore
we can see (in Fig.4.2) that the red dots under the expected value. We notice that the values for
the Bresenham cylinders converges earlier to the correct value compared to a cylinder computed
by the squares. Therefore, modeling a cylinder by the Bresenham algorithm gives better results,
especially with less beads. For a higher number of beads both values converge to the same value.

4.3 Hydrodynamic

We will discuss the results for the hydrodynamic model here, where we have considerd two
differently shaped particles, the first is a simple cuboid.

4.3.1 Friction coefficient of cylinders

To test wether the theory and my model are accurate I first looked at the average friction co-
efficient. The way to compute it, is to first have the velocity vector in the z-direction $\{0, 0, v\}$,
and calculate the friction coefficient in the z-direction. Then, because our cylinder is symmetric
around the z-axis we can tune the velocity in either the x- or the y-direction and calculate the
friction coefficient in the x- and y-direction. We then take the average of the three principal
components of our friction tensor such that we obtain the the mean friction coefficient.

We want to compute the mean friction coefficient for different aspect (length over diameter)
ratios, and therefore we want to scale out the size of our cylinder. This is done by dividing the
mean friction coefficient by the stokes friction coefficient Eq.(2.44) of a sphere with the same
volume as our cylinder. In this way we scale out the size and the viscosity of the fluid.

In a paper by Hansen [5] dating from 2004, he performed an approximation for the friction
coefficient for cylinders with aspect ratios ranging from 0.01 to 100. He performed a truncation
of a series expansion for the friction tensor to calculate the friction coefficient for a model of n
beads that all have the same radius:

$$f = \frac{\sum_{i=1}^{n} \zeta_i}{1 + (6\pi\eta\zeta_i)^{-1} \sum_{i \neq j}^{n} \sum_{j=1}^{n} \zeta_i \zeta_j R_{ij}^{-1}}$$

Together with the Stokes friction coefficient he calculated the hydrodynamic radius (which is
the radius of a sphere with the same fricion coefficient as the calculated particle) for a particle
covered by n beads all having radii σ. Now the particle is not built up out of beads, but only
the surface is covered by beads.

$$R = \frac{n\sigma}{1 + \frac{\sigma}{n} \sum_{i \neq j}^{n} \sum_{j=1}^{n} R_{ij}^{-1}}.$$

The difficulty is now to calculate the double sum in the formula, but in the limit of infinitely
small beads R_{ij} is a chord for the molecule. Denoting the distribution of chords given by the
distance between two arbitrary points on the surface of the molecule by $g(l)$, he could calculate
the double sum,

$$\sum_{i \neq j}^{n} \sum_{j=1}^{n} R_{ij}^{-1} = n^2 \int \frac{g(l)}{l} dl = n^2 < \frac{1}{l} > .$$
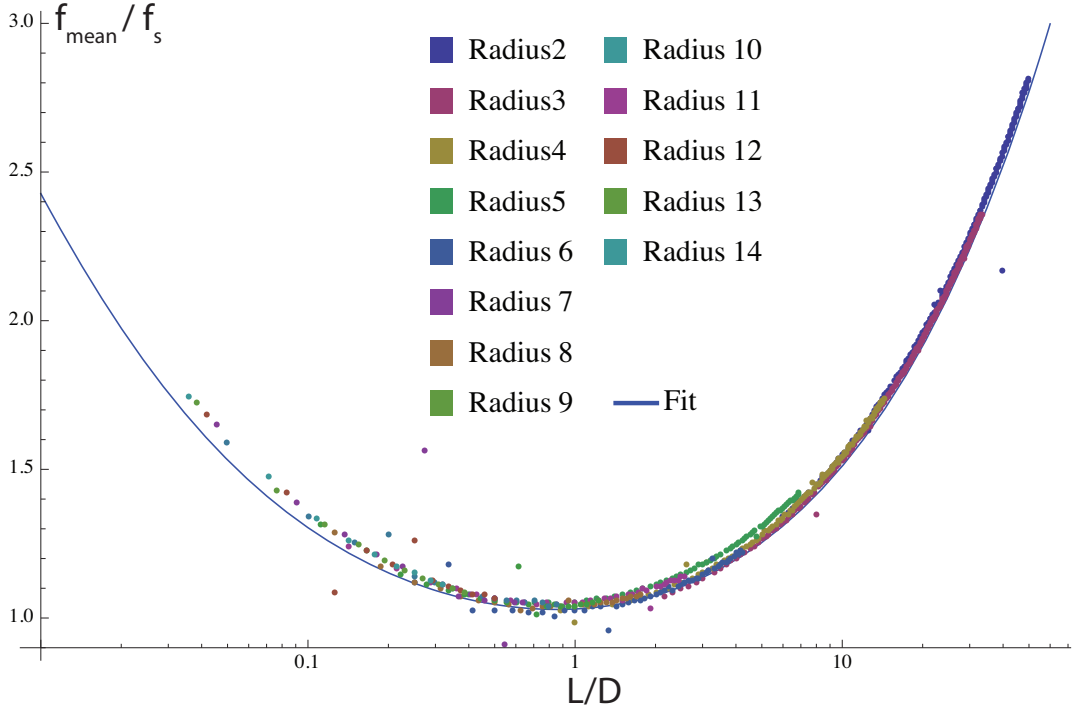
Figure 4.3: *We see on the horizontal axis the aspect ratio ($\frac{L}{D}$) and on the vertical axis the mean friction coefficient (f_{mean}) divided by the friction coefficient of a sphere with the same volume (f_s). In the graph we see the fit from Eq.(4.1) as the blue line. The dots are the data points from the model with Bresenham circles, and we see the different radii of the model, and as we see with increasing radius the circle is modeled better. Again we see that our values are slightly larger than the fit, this is again because we use the Bresenham approximation of a circle.*

Were $< \cdot >$ is the average with respect to distribution g. Inserting this into Eq. (4.3.1) for the hydrodynamic radius one obtains

$$R = \frac{n\sigma}{1 + \frac{\sigma}{n}n^2 < \frac{1}{l} >} \rightarrow < \frac{1}{l} >^{-1} \text{ as } n \rightarrow \infty$$

The results of his paper were then obtained by performing Monte Carlo simulation of the shell of the molecule placing random points in a thin shell on the surface. These points are used to estimate the chord length distribution $g(l)$ from which the hydrodynamic radius and thus friction coefficient were calculated. [5]

He performed above procedure with 10.000 points and 100 cycles for cylinders and fitted his data for the mean friction coefficient divided by the friction coefficient of a sphere with the same volume. The fit is given by;

$$\frac{f_{mean}}{f_s} = 1.0304 + 0.0193x + 0.06229x^2 + 0.00476x^3 + 0.00166x^4 + 2.66*10^{-6}x^7, \quad x \equiv \log(\frac{L}{D}) \quad (4.1)$$

From Fig. 4.3, we see that our model is working correctly and the results fit the approximation of recent papers nicely, especially for lager radii. We can look at the friction coefficient in various
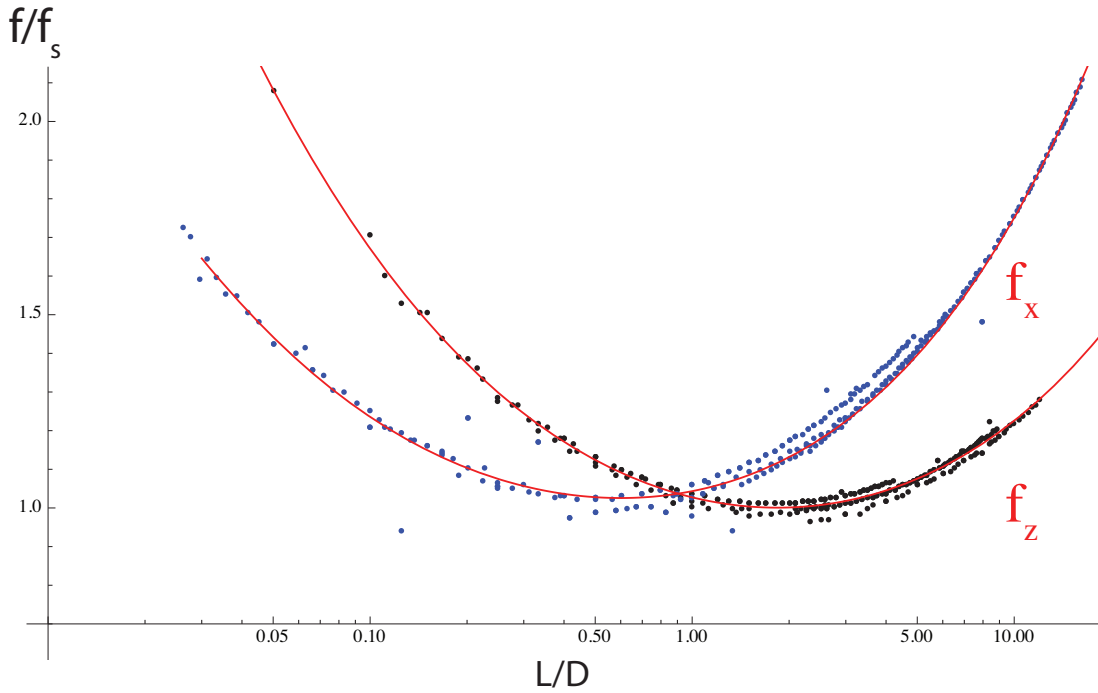
Figure 4.4: *In this figure we see the two different components (f_x and f_y) of the friction tensor for cylinders. Both the x- and z-component follow the same curve, only a bit shifted. In this logplot we have fitted a polynomial in $\log(x)$ and we see that it fits our data correctly. If the cylinder becomes longer we see that the f_x get bigger and if the cylinder becomes shorter than an aspect ratio of 1 the z-component dominates the x-term.*

directions. For a cylinder there are two directions of symmetry to look at. The first is the direction perpendicular to the circle, the second is in the plane of the circle. Since the cylinder is symmetric around the center these two directions determine the friction tensor of the cylinder in the following way:

$$f = \begin{pmatrix} f_x & 0 & 0 \\ 0 & f_y & 0 \\ 0 & 0 & f_z \end{pmatrix}.$$

Since the cylinder is symmetrical around the z-axis we have $f_y = f_x$. We can calculate the different components of the friction tensor by adjusting the velocity of the fluid. For the x or y component we have $\mathbf{v} = \{v, 0, 0\}$ and for the z component we have $\mathbf{v} = \{0, 0, v\}$. In figure 4.4 we plot the two components of the friction tensor.

We can now fit a function through these points so we have an approximation of the friction coefficient per component and we can simply calculate the friction tensor. For the x-component this is given by;

$$\frac{f_x}{f_s} = 1.04317 + 0.0709184x + 0.0748641x^2 + 0.00758238x^3 + 0.0018776x^4 + 3.97684 \times 10^{-6}x^7, \quad x \equiv \log[\frac{L}{D}];$$

and for the z-component by:

$$\frac{f_z}{f_s} = 1.0283 - 0.0865875x + 0.0706047x^2 - 0.00247028x^3 + 0.00181676x^4 + 0.0000251351x^7, \quad x \equiv \log[\frac{L}{D}].$$

We have used the same parameters to fit our data as Hansen did in his Paper [5]. We can see that those lines matches the datapoint accurately between $[0.01; 12]$. For cylinders we can now easily determine the translational friction tensor for aspect ratios between $[0.05; 12]$ and we can use those in other simulations.

4.3.2   Friction coefficient of cuboids

We have seen that the model works correctly for cylinders, but we want to see how the friction tensor changes if we have differently shaped particles. Therefore we now use cuboids ($l \times l \times L$) and compute the friction tensor for these particles. We again have to compute only two components of our tensor, because the x- and y-directions are equivalent. We will compute f_x and f_z in the same way as before, so we divide the friction coefficient by the friction coefficient of a sphere with the same volume. The scale on the x-axis cannot be the same, because we cannot define the radius any more. We therefore chose l/L as the value on the x-axis.

We made a fit to the data points for the interval $[0.4; 2]$, which shows that the lines cross if $\log[x] = 0$, or $L = l$.
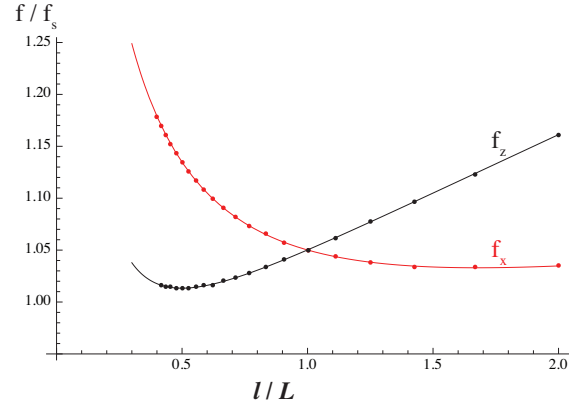

Figure 4.5: *In this graph we see the friction coefficient in the z (Black) and x (Red) direction, with an l of 10 beads. We again see the that the lines cross each other at L = l, as expected, since we have a cube then.*

$$\frac{f_z}{f_s} = 1.0502 + 0.103805x + 0.0733625x^2 + 0.00601893x^3 + 0.0079844x^4, x \equiv \log[\frac{l}{L}]$$

$$\frac{f_x}{f_s} = 1.05012 - 0.0684873x + 0.0725205x^2 - 0.00752809x^3 - 0.000929608x^4, x \equiv \log[\frac{l}{L}]$$

4.3.3   Comparison between cuboids and cylinders

We can compare the results for the two type particles in our hydrodynamic model to see if there is a big difference in the friction tensor. There are some difficulties comparing the two particles, since the particles are of course not shaped the same. The first difficulty is the scale on the x-axis, since the axis is depended on the shape of the particle. Nevertheless we can choose the x-axis in such a way that we can compare the results. For the cuboids we keep the l/L ratio, but for the sphere we take D/L. In this way we scale out the length of our particle and we remain with a constant difference between the axes, because l and D are constant. The value on the z-axis remains the same of course. We can then look at a the individual components and the difference between the components.

In figure 4.6a we see that both the friction components have the same behaviour as we expect. When the particle grows in the z-direction, the friction coefficient for the x-direction gets bigger.
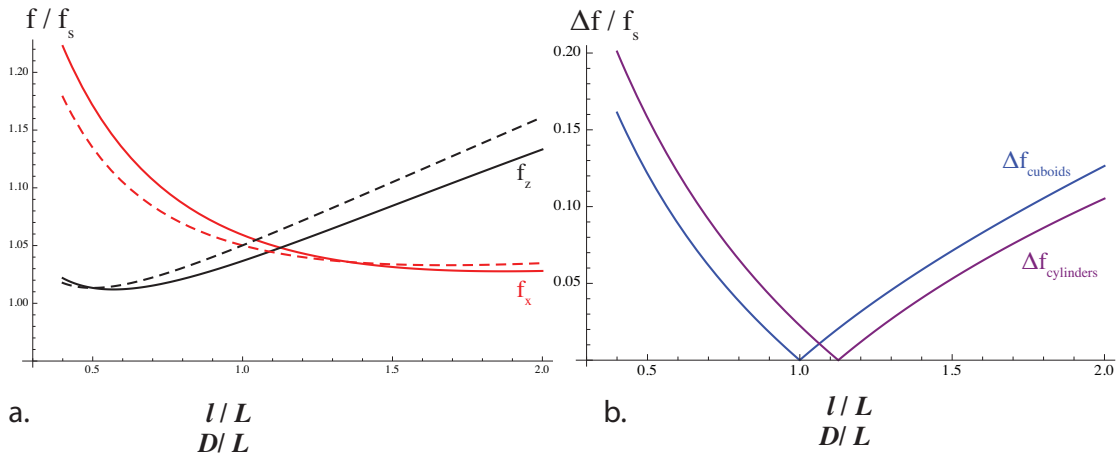
Figure 4.6: **a.** *Graph for the friction coefficients in the x and z component divided by the frictioncoefficient for a sphere with the same volume. The cuboid particles (Dashed, l/L on x-axis) and cylindrical particles (thick lines, D/L on x-axis) are shown in the same graph. For the cylinders we used $D = 10$ and for the cuboids $l = 10$, therefore the scales are the same.* **b.** *Graph of the difference between the two independent components of the friction coefficients of both cylindrical and cuboidal particles.*

The fact that, the friction coefficient gets bigger in the x-direction means that it becomes harder to move in that direction due to the increasing length of the particle. The z component increases just a bit, because our l or D is constant.

4.4   Electrodynamic

We will look at the same particles, but now in the electrodynamic model. We start with the cuboids and show that this model also works correctly, then we will look at cylinders and compare the enhancement factors.

4.4.1   Enhancement factor of cuboids

To test if the electrodynamic model is working correctly I tried to reproduce some of the data the paper by Kwaadgras et al. [6]. In this paper, the authors calculate the polarizability for $(l \times l \times L)$ shaped particles as pictured in Fig.4.7, with $l = 10$ and L ranging from 5 to 100. They used a dimensionless lattice constant ($\tilde{a}$) of 2, because the distance between the atoms is around $5\mathring{A}$ (depended on the molecule) and the atomic polarizability (α_0) is around $10\mathring{A}^3$. Since $\tilde{a} \equiv a/\alpha_0^{\frac{1}{3}}$, we use the dimensionless lattice constant of 2. In the graphs we will plot the fit of our enhancement factor $f_{ii} = \alpha_{ii}/(N\alpha_0)$, the polarisability of our particles divided by the atomic polarisability times the number of dipoles (beads). This enhancement factor shows the influence on the dipoles interacting with each other on the to polarisability when the dipoles are not interacting, such that the total polarizability is the sum of the individual (atomic) polarisabilities. The best fit found on
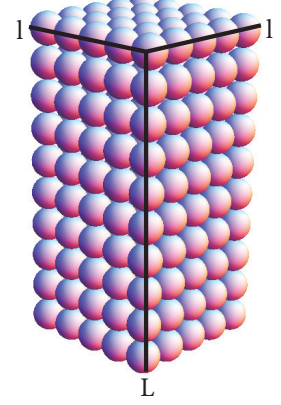

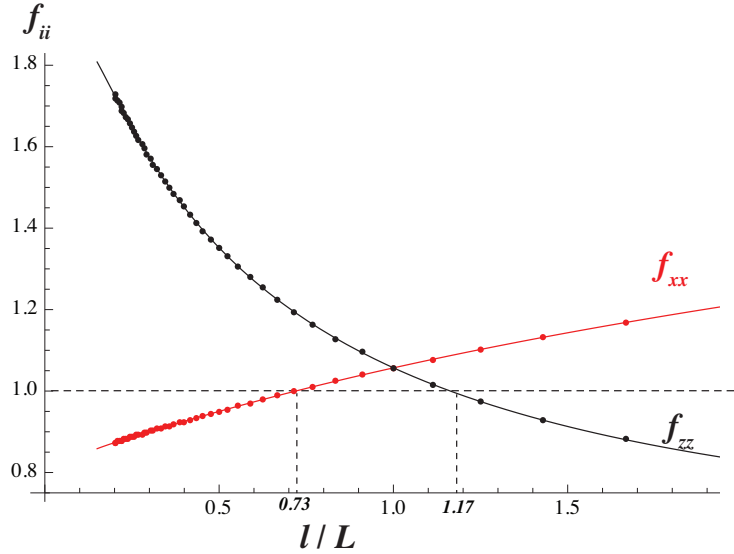Figure 4.7: $l \times l \times L$ shaped particle, here $l = 5$ and $L = 10$.

Figure 4.8: *This figure shows the enhancement factor of the $l \times l \times L$ shaped particles, when the static field is in the i direction. On the horizontal axis we have l/L. From Kwaadgras et al. paper we found that $f_{xx} = 1$ when $l/L = 0.73$ and $f_{zz} = 1$ when $l/L = 1.17$, exactly the values we get out of our data.*

the data points, which we used to make the graphs is;

$$f_{xx} = 1.05689 + 0.190613x + 0.0542399x^2 + 0.000973144x^3 - 0.00195851x^4, x \equiv \log[D/L].$$

$$f_{zz} = 1.05705 - 0.3887x + 0.072942x^2 + 0.02539x^3 - 0.00584069x^4, x \equiv \log[D/L]$$

We see that this data is in good agreement with the data of [6] and the model is working correctly for the electrodynamic case.

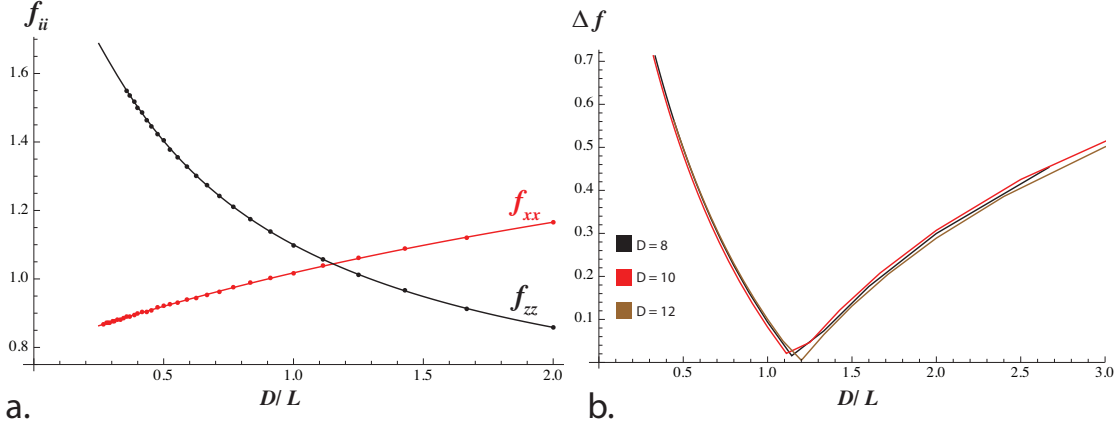### 4.4.2 Enhancement factor of cylinders

a.

b.

Figure 4.9: **a.** *This figure shows the plot of the fit of the enhancement factor of the cylindrical shaped particles. We have used $D = 10$ for the calculations.* **b.** *Here we see the difference between the two enhancement factors ($|f_{xx} - f_{zz}|$). We see that the different number of beads, or the different values of D have no effect on the difference between the ehancementfactor.*

Since we now know that our model is working correctly, we can continue with other spaped particles, for instance the cylindrical shaped particles so we can compare them to the hydrodynamic case. We will now again use the dimensionless lattice constant of 2 to build up the particle. We will only use the Bresenham circle algorithm to compute the bead positions within the particles, since the best results in hydrodynamic were obtained that way.

The fits for the enhancement factor of the cylindrical shaped particles, we found again for the best fit a logarithmic polynomial.

$$f_{xx} = 1.01773 + 0.176491x + 0.0534726x^2 + 0.00146695x^3 - 0.00234464x^4, x \equiv \log[D/L],$$
$$f_{zz} = 1.09976 - 0.40415x + 0.0696706x^2 + 0.0242134x^3 - 0.0113715x^4, x \equiv \log[D/L].$$

4.4.3 Cuboid versus Cylinder

Next we can compare the results for the enhancement factor of the two differently shaped particles. We will perform the comparison in the same way as we did in hydrodynamics, so we can subsequently compare the results of both hydrodynamics and electrodynamics next.

4.5 Comparison between the data

It is hard to compare the hydrodynamic and electrodynamic data to each other, because they have different units. Nevertheless we try to compare the results for the friction coefficient and
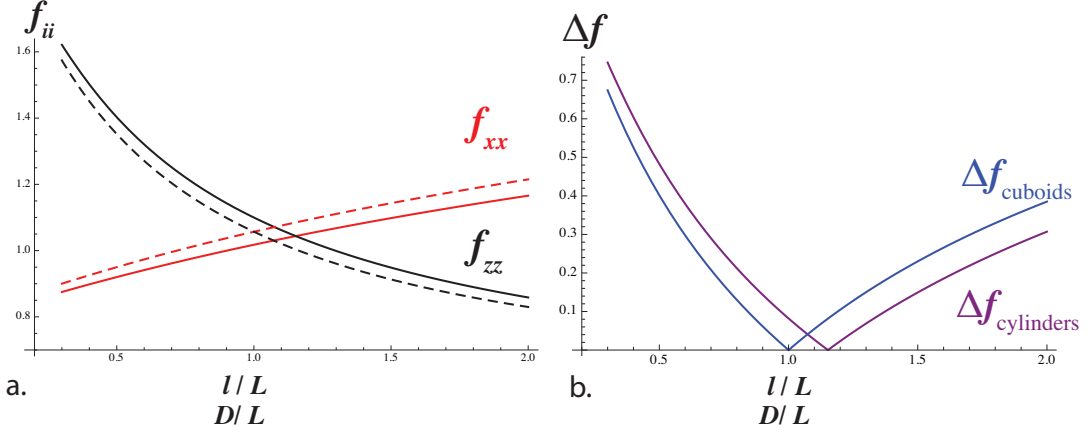
Figure 4.10: **a.** *The different enhancement factor elements, dashed the cuboid-shaped particles and the solid line represents the cylinder-shaped particles. They almost overlap, which shows that the enhancement factor for a cylinder or a cuboid are pretty much the same.* **b.** *The difference between the enhancement factor elements ($\Delta f = |f_{xx} - f_{zz}|$) of both the cuboidal and the cylindrical shaped particle. We see that they do not overlap, because the particles are differently shaped. Nevertheless the distance between the two graph's is almost constant, so the difference in enhancement factors is constant and they follow the same corve, but a bit shifted.*

the enhancement factor for both cuboids and cylinder-shaped particles.

We showed the results for the friction coefficient and the enhancement factor for cuboids in the previous sections. I have combined these results for both the cuboids and the cylinders in Fig. 4.11. We see that the x-component from the friction coefficient for an l/L ratios bigger than 1.2 is smaller than the z component. For the enhancement factor it is the other way around. There the x-component for l/L ratios bigger than 1 is smaller than the z-component of the enhancement factor. We can explain this by looking at the meaning of the friction coefficient and enhancement factor.
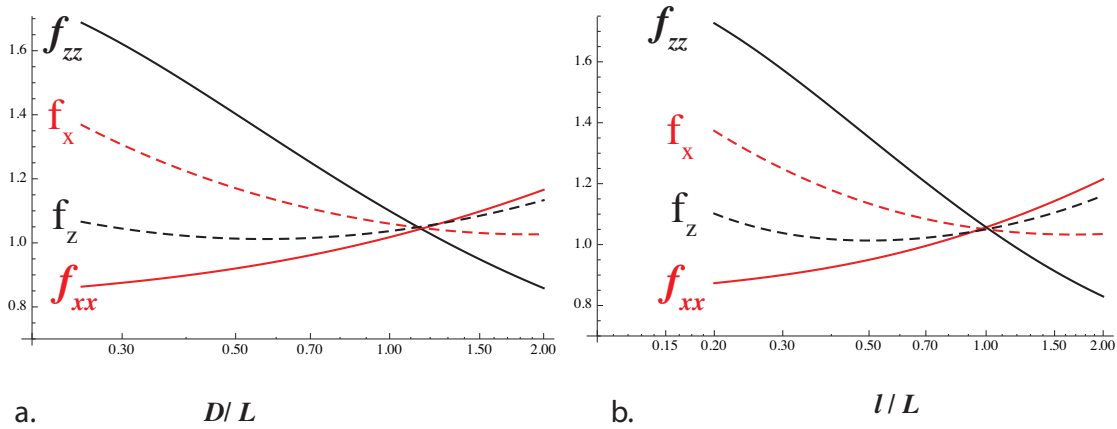
Figure 4.11: **a.** *Here we see the hydrodynamic and electrodynamic model for cylindrical shaped particles. The solid line represents the coupled dipole method and the dashed line the bead model system.* **b.** *Again the hydrodynamic and electrodynamic model, but know for cuboid shaped particles.*

Friction coeffcicient

If we look at figure 4.11 we see the two components for the friction tensor. We expect that the friction coefficient increases when the x-component, or when the length (L) increases, and thus L/D increases. If we move the particle in the x-direction through the fluid, we expect the friction to increase if we have a longer cylinder. Furthermore we have the relationship $D \propto f^{-1}$, so the particle will diffuse less in the x-direction. This can be observed in experiments by tracking the particles in Brownian motion. For the z-component the length is of less influence, so for a constant D it should be almost the same. If however the aspect ratio becomes small (< 1), both the surfaces start to grow and the friction coefficients goes up as we can see in the graph.

Enhancement coeffcicient

As we can see in figure 4.11, the enhancement factor of f_{zz} grows fast if the ratio l/L decreases. This is what we expect, because if we apply an electric field in a random direction the cylinder will obey the simple relation $\mathbf{E}_0 = \alpha\mathbf{p}$ as we saw in the theory. From electrodynamics we know that an applied electric field on a particle causes the particle to induce an electric field opposite to the electric field. If we look at the enhancement factor which is proportional to the polarizability we get the largest field when the particle aligns in the direction where the enhancement factor is the biggest, in our case that will be in the z direction. From experiments we know that rods (which look quite similar to cylinders or cuboids with small l/L or D/L ratios) do align in the z direction with a constant electric field. Therefore the z-component of the polarizability should be the biggest for a rod-like particle.

Chapter 5

Conclusion and Outlook

The aim of this bachelor project is to find a relationship between electrodynamics and hydrodynamics so we could use the results of the coupled dipole method for the friction tensor. In the theory section we see that there is indeed an analogy for the coupled dipole method in hydrodynamics, which I call the bead model. We see that we can make direct analogies between the force and the dipole moment ($\mathbf{F} \equiv \mathbf{p}$) and the static electric field and the velocity ($\mathbf{v} \equiv \mathbf{E}_0$) for the translational component of the friction tensor and polarisability.

Hydrodynamic

$$\mathbb{T}_{ii} = \frac{1}{6\pi\eta|r_i|}\mathbb{1}$$

$$\mathbb{T}_{ij} = \frac{1}{8\pi\eta|r_{i,j}|}\left(\mathbb{1} + \frac{\mathbf{r}_{i,j}\mathbf{r}_{i,j}^t}{|r_{i,j}|^2}\right)$$

Electrodynamic

$$\mathbb{T}_{ii}^* = \frac{1}{E_0\alpha_0}\mathbb{1}$$

$$\mathbb{T}_{i,j}^* = \frac{1}{E_0|r_{i,j}|^3}\left(\mathbb{1} - \frac{3\mathbf{r}_{i,j}\mathbf{r}_{i,j}^t}{|r_{i,j}|^2}\right)$$

Futhermore we can compare the different interaction tensors to each other, since that is the only difference between the two models. We see that in the hydrodynamic case both term have the same sign and in electrodynamics there is a difference in signs. On top of that we have the difference that the electrodynamic interaction tensor goes as r^{-3} and the hydrodynamic model goes as r^{-1}. Therefore we cannot copy the results directly from the coupled dipole method.
We made a model for both the electrodynamic and hydrodynamic situation where we only change the interaction tensors. We have compared the results to two papers [5] and [6] to see whether our model was working correctly, and it did. We see however that the results for hydrodynamics and electrodynamics, as presented in chapter 4, do not mach and we therefore cannot copy the results from the coupled dipole method directly to the translational friction tensor. We showed however that the difference between the models is just the interaction tensor and we can copy the models used for the coupled dipole method. We only have to replace the electrodynamic interaction tensor by the hydrodynamic interaction tensor. This way we can compute the translational friction tensor quickly without doing much new work.

5.1   Outlook

In this bachelor project I have just looked at the translational friction coefficient, therefore we could make the analogy between the velocity and the static electric field. The beads can only move in the same direction, because the particle cannot rotate. In experiments particles do rotate and it would be a good idea to look at the rotational friction tensor and even at the relation between the translational and rotational friction tensors. It is hard to keep making the comparison between the electrodynamics and hydrodynamics there, since there is no rotational

polarizability in electrodynamics, ($\nabla \times \mathbf{E} = \mathbf{0}$). We can however adjust the bead model system to calculate the rotational friction tensor and we might use the same techniques that are used in the coupled dipole method. If we have a model for both the translational and rotational friction tensor we can start looking at different type of particles and see how the friction tensors change with the change in shape.

Bibliography

[1] Peidong Yang Andrea R. Tao, Susan Habas. Shape control of colloidal metal nanocrystals. *Small*, 4, 2008.

[2] David C. Teller Eric Swanson and Christoph de Haen. The low reynolds number translational friction of ellipsoids, cylinders, dumbbells, and hollow spherical caps. numerical testing of the validity of the modified oseen tensor in computing the friction of objects modeled as beads on a shell. *Journal of Chemical Physics*, 68, 1978.

[3] Hye-Young Kim et al. Static polarizabilities of dielectric nanoclusters. *Physical Review Letters A*, 72, 2005.

[4] David J. Griffiths. *Introduction to electrodynamics*. Pearson, 2008. p141-p143, p155, p186 - p188.

[5] Steen Hansen. Translational friction coefficients for cylinders of arbitrary axial estimated by monte carlo simulations. *Journal of Chemical Physics*, 121, 2004.

[6] Bas Kwaadgras. Polarizability and alignment of dielectric nanoparticles in an external electric field: Bowls, dumbbells, and cuboids. *Journal of Chemical Physics*, 135, 2011.

[7] Landau and Lifshitz. *Fluid Dynamics*. ButterworthHeinemann, 1987.

[8] Julius Adams Stratton. *Electromagnetic Theory*. John Wiley and Sons Ltd, 2007. P204 - p209.

[9] Maria M. Tirado and Jose Garcia de la Torre. Translational friction coefficients of rigid, symmetric top macromolecules. application to circular cylinders. *Journal of Chemical Physics*, 71, 1979.